DOI 10.1007/s10812-018-0670-0
Journal of Applied Spectroscopy, Vol. 85, No. 3, July, 2018 (Russian Original Vol. 85, No. 3, May–June, 2018)

USE OF FOURIER TRANSFORM IR SPECTROSCOPY FOR THE STUDY OF SALIVA COMPOSITION

L. V. Bel'skaya,[a,b*] E. A. Sarf,[b] and N. A. Makarova[c]

UDC 543.422:612.313.1

The IR spectrum of saliva may be divided into groups of absorption bands corresponding to lipids, proteins, nucleic acids, and sugars. The finding of thiocyanate ion absorption bands is a characteristic feature of the spectra of saliva. In comparing a typical IR spectrum of saliva with the spectra of albumin, glucose, and lysozyme, a similarity is noted at 1100–1040 cm^{-1} with the spectrum of albumin and at 1700–1400 cm^{-1} with the spectra of glucose and lysozyme. It was shown that sugars are found in saliva in a form bound with proteins. Correlations were found between band intensities in the IR spectrum of saliva and its biochemical composition.

Keywords: *saliva, FTIR spectroscopy, biochemical composition of saliva.*

Introduction: There has been increasing recent interest in the study of human saliva as a material with unique properties and diagnostic potential [1, 2]. The study of saliva involves noninvasive methods and is carried out to determine age and physiological status, to discover somatic disease, pathology of the saliva glands and oral tissues, genetic markers, and to monitor drugs [3–5].

Saliva contains a variety of biological molecules, including DNA, matrix RNA, microRNA, proteins, metabolites and microbiota. Change in the concentration of these components may reveal systemic disease, earlystage disease in the oral cavity as well as to obtain disease prognosis and to monitor the response to treatment [6]. Salivaomics was proposed as term in 2008 encompassing knowledge of the various saliva components, including the genome, epigenome, transcriptome, proteome, metabolome, and microbiome [7, 8].

Promise is found for the use of various spectral methods for the study of saliva composition [9, 10], in particular, Fourier transform IR spectroscopy, which is a method of vibrational spectroscopy that can be used for qualitative and structural analysis and the determination of structural changes in organic molecules [11, 12]. This method is a powerful tool for analysis of biological samples such as plasma, blood serum, tissues, and urine [13–15] and has already been proposed as a supplemental method in clinical laboratory diagnostics for characterizing various diseases [16, 17], including those for which early diagnosis is an important diagnostic factor [18–21].

The IR spectroscopy of saliva presently has found little use for the diagnosis of disease of the oral cavity [22, 23]. Information has been obtained in several studies involving the quantitative analysis of the biochemical components of saliva in real time without the use of reagents [24, 25]. Quantitative analysis using IR absorption bands in the range 4000–700 cm^{-1} has revealed specific absorption bands of proteins, glucose, urea, secretory immunoglobulin A (sIgA), cortisol, and phosphates [26]. We should note that there have been almost no systematic data on the functional group composition of saliva in normal individuals or in patients with various diseases.

In the present work, we determined the qualitative functional group composition of human saliva in the norm using IR spectroscopy.

Materials and Methods. A group of 40 healthy volunteers (20 men, 20 women, age 23.1 ± 0.9 years) participated in this study. The criteria for inclusion were lack of symptoms of active infection (including suppuration) and dental prophylaxis. The saliva samples were collected over 24 h every 3 h (at 3, 6, 9, 12, 15, 18, 21, and 24 h) over 10 min followed by centrifugation at 7000 rpm. For all samples, we determined the salivation rate, pH, concentrations of calcium, potassium,

*To whom correspondence should be addressed.

[a]Omsk State Technical University, 11 Mir Ave., Omsk, 644050, Russia; email: ludab2005@mail.ru; [b]KhimServis LLC, Moscow, Russia; [c]Omsk State Pedagogical University, Omsk, Russia. Translated from Zhurnal Prikladnoi Spektroskopii, Vol. 85, No. 3, pp. 436–442, May–June, 2018. Original article submitted August 11, 2017.

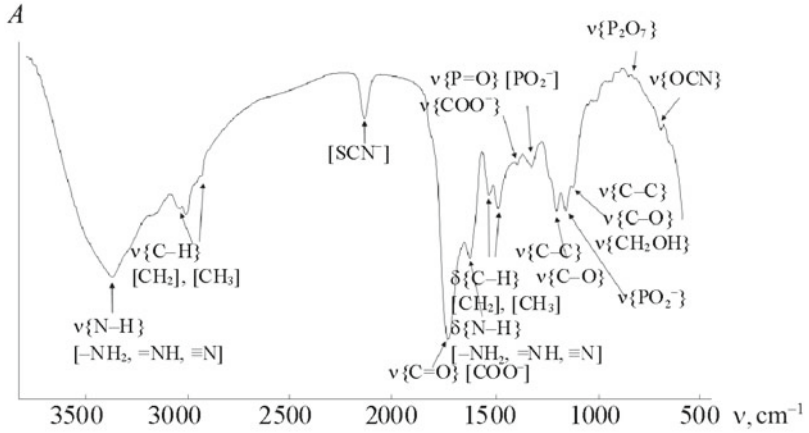

Fig. 1. IR spectrum of normal saliva.

sodium and inorganic phosphorus ions using a Lumex Capel 105M capillary electrophoresis system (St. Petersburg) and then calculated the Ca/P and Na/K coefficients.

In addition, 50 mL saliva samples were dried for 30 min on a zinc selenide plate in a thermostat at 37°C. The IR absorption spectra were taken on a Simex FT801 Fourier transform IR spectrometer at 500–4000 cm^{-1} using 32 scans; the resolution was 4 cm^{-1}.

Statistical analysis of the data was carried out using the StatSoft Statistica 10.0 programs by a nonparametric method using the Wilcoxon signedrank test for dependent groups (Mann–Whitney *U* test). The sample was described using calculation of the median (Me) and interquartile range as the 25th and 75th percentiles (LQ, UQ). The differences were considered statistically significant at $p < 0.05$. The correlation analysis was carried out by the Spearman method.

Results and Discussion. A typical IR spectrum of saliva is given in Fig. 1. There are three major groups of macromolecules: lipids (3000–2800 cm^{-1}), proteins (1700–1600 and 1560–1500 cm^{-1}), and nucleic acids (1250–1000 cm^{-1}). The broad band at 3273 cm^{-1} corresponds to amide A. The mediumintensity narrow band at 2057 cm^{-1} corresponds to thiocyanate (SCN^-) anions. This band is characteristic specifically for saliva and is seen in a region, which usually does not contain absorption peaks attributed to biological samples [27–29]. Comparison with the IR spectra of blood plasma, sperm, and vaginal secretion showed that the thiocyanate anion band is observed only in the IR spectra of saliva although the intensity may change due to natural fluctuations in the concentration of this anion [30]. The narrow bands at 1649 and 1543 cm^{-1} can be classified as amide I and II. The band at 1075 cm^{-1} in the saliva spectra corresponds to sugar fragments.

The remaining strong absorption bands correspond to the methylene groups of the sidechains of amino acids in proteins and lipids (1452 cm^{-1}), sidechains of amino acids (1396 cm^{-1}), amide III/phospholipids (1286–1320 cm^{-1}), and fragments of sugars, glycosylated proteins, and nucleic acid phosphate groups (1080–950 cm^{-1}). The bands corresponding to various chemical groups are described in greater detail in Table 1.

Orphanou [14] compared the IR spectra of aamides and saliva and found an overlap of maxima in the region of sugar absorption. Thus, the bands at 1080–950 cm^{-1} may be assigned to glycosylated α-amidase as well as to other residues of sugars present in saliva. We compared the IR spectrum of saliva with the spectra of albumin, glucose, and lysozyme (Fig. 2).

Albumin is the predominant protein in saliva. According to our data, the average albumin concentration is 0.259 mmole/L [0.169, 0.394]. It would be logical to assume that the bands at 1650 and 1540 cm^{-1} corresponding to amide I and amide II are a consequence of the presence of albumin [39]. It is precisely this region, which is similar for saliva and blood plasma [14]. The remaining bands in the IR spectrum of blood plasma are classified as weak due to their low intensities. These bands correspond to plasma lipids (2956 cm^{-1}), sidechains of amino acids, lipids, and proteins (1456 cm^{-1}), sidechains of fibrinogen (1395 cm^{-1}), amide III (1286–1320 cm^{-1}), and carbohydrates such as glucose (1250–925 cm^{-1}).

Comparison of the IR spectrum of saliva with the glucose spectrum revealed a correspondence of bands at 1030–1100 cm^{-1} (Fig. 2b). However, the presence of bands in the IR spectrum of glucose at 638, 2048, and 2185 cm^{-1}, which are lacking in the absorption spectrum of saliva, indicates that carbohydrates are found in saliva in bound form, predominantly with proteins. Thus, the IR spectrum of saliva was compared with the spectrum of lysozyme (Fig. 2c). The IR spectrum of lysozyme has bands at 1040–1100 cm^{-1}, which correspond to glycosylated proteins as well as at 1375 and 1419 cm^{-1}, which

TABLE 1. Major Absorption Bands (cm^{-1}) in the IR Spectra of Saliva

Present work	Vibration type	Interpretation	References
3282	νNH	Amide A	3270–3285 [31]
3065	R-NH_2 ($\nu_{as}NH$, ν_sNH) R-NH (νNH)	Primary and secondary amides	3067 [32]
2926, 2850	νCH_2, νCH_3	Methylene groups of mucus membrane lipids	2875, 2933 [33]
2059	νSCN^-	Thiocyanates	2058 [29]
1645–1650	νCO	Amide I	1645 [34, 35]
1544	δNH, νCN	Amide II	1548 [34, 35]
1452, 1393	δCH_2, δCH_3	Methylene groups of sidechains of amino acids, lipids and proteins	1450, 1395–1410 [34, 35]
1260–1300	δNH, νCN	Amide III	1270 [34, 35]
1240–1245	$\nu_{as}PO$	Phospholipids	1244 [36]
1121	ν_sPO, νCC, νCO	Phospholipids, RNA, sugars	1125 [27]
1075	νCN, $\nu_sPO_2^-$	DNA, RNA	1078 [27]
1037	νCC, νCO, νCH_2OH	Sugars, glycosylated proteins	950–1080 [37]
735–775	$\nu PO(P_2O_7)$	Oligo and polysaccharides, phosphatases, phospholipids	735–775 [38]
625–765	δOCN	Amide IV	625–765 [38]
640–800	δNH	Amide V	640–800 [38]
535–605	δCO	Amide VI	535–605 [38]

Note: stretching vibrations: ν_s) symmetrical, ν_{as}) asymmetrical, δ) deformation vibrations.

correspond to methyl group vibrations in the lysozyme molecule. Mediumintensity bands are observed in this spectral region also for saliva. Thus, lysozyme may be a common dominant component found in the spectra of saliva, which is supported by the overlap of the peaks of sidechains of amide II and amino acids [24].

Some of the biochemical components of saliva have specific IR bands [32, 40]. Khaustova et al. [24] have shown that the intensities of the bands at 1503–1440, 1317–1249, and 1190–936 cm^{-1} correlate strongly with the levels of common saliva proteins. The regions 1567–1526 and 1488–1406 cm^{-1} correlate with the concentration of sIgA, while the regions 1943–1526, 1391–1249, and 1115–973 cm^{-1} correlate with the concentration of cortisol and the regions 1578–1548, 1526–1496, and 1444–1305 cm^{-1} correspond with the α-amidase activity.

IR spectra were taken for saliva samples over 24 h at intervals of 3 h. These spectra were compared relative to the intensity of the bands corresponding to the major groups of macromolecules, namely, lipids (3000–2800 cm^{-1}), proteins (1700–1600 and 1560–1500 cm^{-1}), and nucleic acids (1250–1000 cm^{-1}). This procedure permitted us to combine the samples into two groups collected during the day and during the night (Fig. 3). In accord with the similar characteristics of the IR spectra, we calculated the medians and interquartile ranges of the biochemical parameters as well as the intensities of the bands corresponding to the major functional groups of the saliva components (Fig. 3, Table 2). The intensities of the bands corresponding to sugar residues in glycoproteins (1075 cm^{-1}) and amino acid residues (1547 cm^{-1}) increase during the daytime while the intensity of the bands of oral cavity mucus membrane lipids (2963 cm^{-1}) and free amino groups (3287 cm^{-1}) decrease. Calculation of the Spearman correlation coefficients confirms the existence of a correlation between the protein content in saliva and the intensities of the bands at 1547 and 3287 cm^{-1} ($R = 0.7143$ and $R = 0.7173$). Presumably, the increase in the intensities of the bands characteristic for sugars and amino acids is related to the ingestion of these substances in food, while lipids largely enter the saliva from the cell membranes of the oral cavity mucus membrane by the metabolic action of the microflora at night.

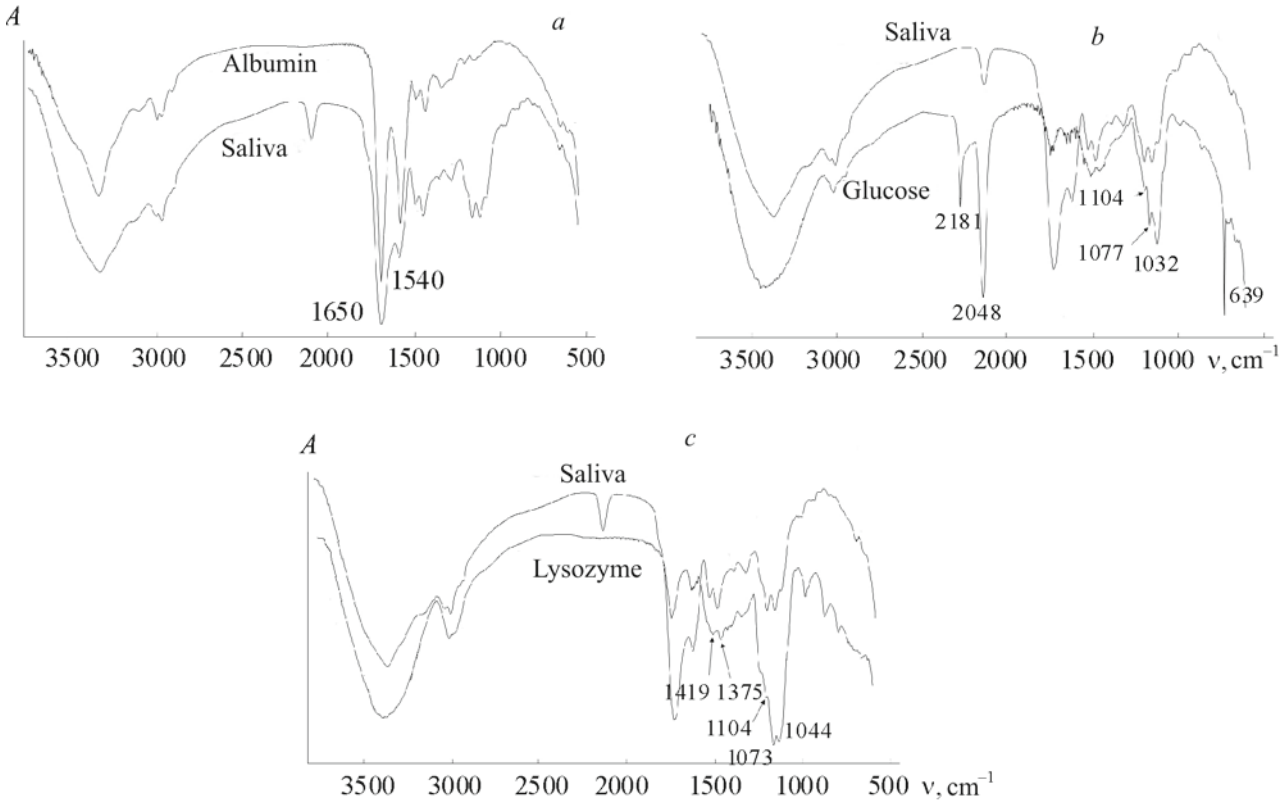

Fig. 2. Comparison of the IR spectra of saliva and albumin (a), glucose (b), and lysozyme (c).

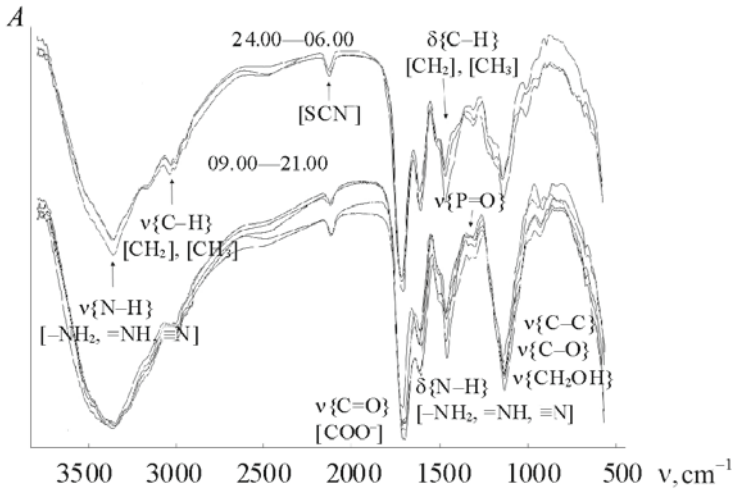

Fig. 4. IR spectra of the saliva of patients with breast cancer (a) and bladder cancer (b).

These features of the IR spectra of saliva were found to correlate with the results of biochemical analysis (Table 2). Thus, increased intensity of the band at 1075 cm^{-1} indicates a strong negative correlation with the amount of total protein (R = –0.9524). A positive correlation is noted with acidity of the medium (R = 0.7795) and a negative correlation is noted with the sodium (R = –0.7143) and phosphorus contents (R = –0.7381). The mineralizing function of saliva is largely due to supersaturation of Ca^{2+} and HPO_4^{2-} anions. The major mechanism for the maintenance of the supersaturation of saliva by these ions is their micellar state. The micelle core consists of $Ca_3(PO_4)_2$. The potentialdetermining ions are HPO_4^{2-} and the counterions are Ca^{2+} (however, these are located in the diffuse layer). The micelles in saliva are protected from aggregation

TABLE 2. Biochemical Composition and Intensities of Absorption Bands of Saliva during Daytime and Nighttime

Index	24:00–06:00	09:00–21:00	*p*
pH	6.52 [6.49; 6.62]	7.00 [7.00; 7.01]	0.0245
Total proteins, mg/L	0.86 [0.78; 1.21]	0.35 [0.31; 0.41]	0.0526
Salivation rate, mL/min	0.74 [0.45; 0.77]	1.10 [1.04; 1.25]	0.0213
Ca/P	0.311 [0.254; 0.416]	0.267 [0.217; 0.351]	0.6547
Na/K	1.059 [0.840; 1.309]	0.622 [0.531; 0.634]	0.0271
Intensity, %			
1075 cm^{-1}	25.5 [13.8; 42.3]	63.1 [61.5; 68.1]	0.0154
1243 cm^{-1}	3.9 [2.6; 5.3]	3.0 [1.6; 3.5]	0.1797
1403 cm^{-1}	17.5 [14.7; 40.2]	24.2 [14.5; 33.2]	0.6547
1547 $см^{-1}$	27.2 [23.9; 29.0]	47.6 [32.0; 50.9]	0.0253
1648 cm^{-1}	60.6 [15.0; 65.1]	51.3 [32.6; 59.9]	0.4561
2060 cm^{-1}	6.9 [6.1; 7.9]	6.2 [4.4; 6.3]	0.2967
2963 cm^{-1}	2.6 [2.2; 2.6]	1.2 [0.6; 1.6]	0.0339
3287 cm^{-1}	19.2 [16.9; 36.9]	14.7 [12.6; 15.3]	0.0353

mainly by the glycoprotein, mucin, which, due to its high surface activity, can be adsorbed on colloidal particles and display a protective effect. A significant increase in the concentration of the dominant saliva cations (sodium and potassium) leads to weakening of the protective properties of the biopolymers due to destruction of the hydrate shells of the glycoprotein macromolecules and their denaturation. On the other hand, an increase in the pH of the medium leads to increased stability of the calcium phosphate micelles and, hence, a higher level of carbohydratecontaining proteins in saliva. Therefore, the protective properties of saliva glycoproteins may be indirectly evaluated relative to the intensity of the band at 1075 cm^{-1}, which, in turn, provides information on the mineralizing potential of saliva.

The intensity of the band corresponding to phospholipids (1243 cm^{-1}) was found to correlate with the calcium concentration, which apparently is a consequence of complex formation between these saliva components (R = 0.6429). Additional evidence is also found in the positive correlation of the calcium level and intensity of the band at 2963 cm^{-1} (R = 0.6786). It is interesting to note the existence of a negative correlation between the salivation rate and the contents of proteins and lipids in saliva (1547, 2963, and 3287 cm^{-1}), while an enhanced salivation rate correlates with an increased levels of sugars (1075 cm^{-1}, R = 0.6905).

We should note the internal correlation between the intensities of the individual absorption bands in the IR spectrum of saliva. Thus, the bands of amides and sugars show a negative correlation, while the structural fragments of amides (for example, 1547 and 3287 cm^{-1}) show a positive correlation (R = 0.7143). The C=O bond stretching vibrations correlate with the level of phospholipids (1243 cm^{-1}) and the methylene groups of the sidechains of amino acids, lipids, and proteins (1403 cm^{-1}). On the whole, calculation of the ratios of the intensities (areas) of the bands of the different functional groups potentially may be informative.

Significant differences are found in the IR spectra of saliva in the case of a number of systemic diseases of humans, in particular, cancer. This feature opens prospects for the use of this method for the diagnosis of disease. As an example, IR spectra of samples of saliva from breast and bladder cancer patients are given in Fig. 4. The conformational structure of protein is altered in both cases, which is seen in a lower intensity of the amide II band (1544 cm^{-1}). Changes in the secondary structure of proteins due to hypomethylation are manifest in an increase in ratio of the intensities of the bands at 1398 and 1454 cm^{-1} (1398/1454 cm^{-1}). Higher cell activity (band at 968 cm^{-1}) also indicates tumor growth. This band is characteristic for both these IR spectra but is virtually absent in the saliva spectra of normal individuals (Fig. 1). An additional difference in the IR spectrum of the bladder cancer patient is the presence of bands at 679, 742, 834, and 1330 cm^{-1} (Fig. 4b).

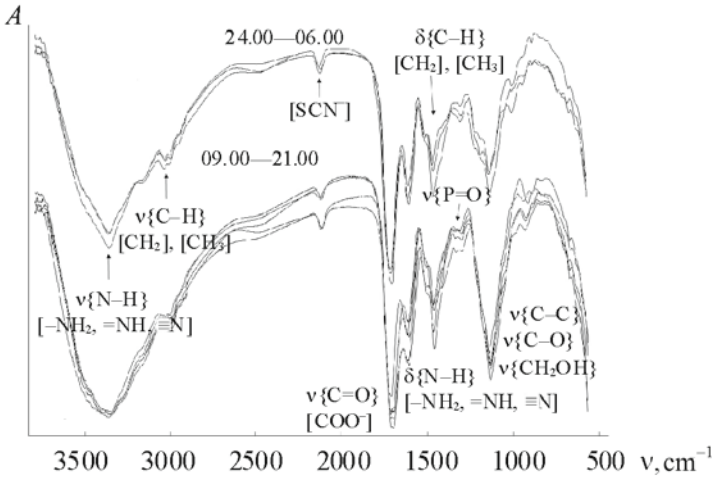

Fig. 3. IR spectra of the saliva of patients with breast cancer (a) and bladder cancer (b).

Conclusions. The qualitative functional group composition of human saliva has been determined. Groups of absorption bands may be discerned in the IR spectrum of saliva, corresponding to lipids, proteins, nucleic acids, and sugars. A special feature of saliva spectra is the presence of thiocyanate ion absorption bands. Comparison of a typical IR spectrum of saliva with the spectra of albumin, glucose, and lysozyme shows similarities at 1700–1400 cm^{-1} with the albumin spectrum and at 1100–1040 cm^{-1} with the spectra of glucose and lysozyme. Correlations were found between the intensities of the bands in the IR spectrum of saliva and its biochemical composition. The existence of internal correlations in the IR spectrum suggests an equilibrium between the individual functional groups in normal individuals. Departure from this equilibrium may characterize various pathological states in the human organism.

REFERENCES

1. H. Zhang, X. Sun, and X. Wang, *Appl. Biochem. Biotechnol.*, **168**, 1718–1727 (2012).
2. E. V. Kochurova, *Klinich. Lab. Diagnostika*, **1**, 13–16 (2014).
3. S. A. Khaustova, M. Yu. Shkurnikov, E. S. Grebenyuk, V. G. Artyushenko, and A. G. Tonevitskii, *Byul. Éksper. Biol. Med.*, **148**, No. 11, 597–600 (2009).
4. E. Papacosta and G. P. Nassis, *J. Sci. Med. Sport*, **14**, 424–434 (2011).
5. S. Chiappin, G. Antonelli, R. E. F. Gatti, and E. F. De Palo, *Clinic. Chim. Acta*, **383**, 30–40 (2007).
6. S. Bandhakavi, M. D. Stone, G. Onsongo, S. K. Van Riper, and T. J. Griffin, *J. Proteome Res.*, **8**, 5590–5600 (2009).
7. J. A. Loo, W. Yan, P. Ramachandran, and D. T. Wong, *J. Dent. Res.*, **89**, 1016–1023 (2010).
8. Y. Goswami, R. Mishra, A. P. Agrawal, and L. A. Agrawal, *IOSR J. Dental Med. Sci.*, **14**, No. 3, 80–87 (2015).
9. G. M. Zubareva, V. M. Mikin, G. E. Bordina, I. A. Belyaeva, N. P. Lopina, S. M. Zubarev, and A. V. Kargapolov, *Stomatologiya*, **5**, 7–10 (2009).
10. P. Seredin, D. Goloschapov, V. Kashkarov, Y. Ippolitov, and K. Bamberry, *Results in Physics*, **6**, 35–321 (2016).
11. O. G. Ildiz, H. Arslan, O. Unsalan, C. Araujo-Andrade, E. Kurt, H. T. Karatepe, A. Yilmaz, O. B. Yalcinkaya, and H. Herken, *Spectrochim. Acta A: Mol. Biomol. Spectrosc.*, **152**, 551–556 (2015).
12. F. Zapata, M. A. F. de La Ossa, and C. García-Ruiz, *TrAC Trends Anal. Chem.*, **64**, 53–63 (2015).
13. A. S. Gordetsov, *Sovr. Tekhnol. Meditsine*, **1**, 84–98 (2010).
14. C. M. Orphanou, *Forens. Sci. Int.*, **252**, 10–16 (2015).
15. I. Gregório, F. Zapata, and C. García-Ruiz, *Talanta*, **162**, 634–640 (2017).
16. A. L. Mitchell, K. B. Gajjar, G. Theophilou, F. L. Martin, and P. L. MartinHirsch, *J. Biophoton.*, **7**, 153–165 (2014).
17. L. Sitole, F. Steffens, T. P. J. Krüger, and D. Meyer, *J. Integr. Biol.*, **18**, 513–523 (2014), doi: 10.1089/omi.2013.0157.
18. A. S. Peters, J. Backhaus, A. Pfützner, M. Raster, G. Burgard, S. Demirel, D. Böckler, and M. Hakimi, *Vibr. Spectrosc.*, **92**, 20–26 (2017).
19. M. Khanmohammadi, K. Ghasemi, A. B. Garmarudi, and M. Ramin, *Spectrochim. Acta A: Mol. Biomol. Spectrosc.*, **136**, 1782–1785 (2015).

20. F. Elmi, A. F. Movaghar, M. M. Elmi, H. Alinezhad, and N. Nikbakhsh, *Spectrochim. Acta A: Mol. Biomol. Spectrosc.*, **187**, 87–91 (2017).
21. X. Wang, X. Shen, D. Sheng, X. Chen, and X. Liu, *Spectrochim. Acta A: Mol. Biomol. Spectrosc.*, **122**, 193–197 (2014).
22. E. Giorgini, P. Balercia, C. Conti, P. Ferraris, S. Sabbatini, C. Rubini, and G. Tosi, *J. Mol. Struct.*, **1051**, 226–232 (2013).
23. H. K. Yip and W. M. To, *Dental Mater.*, **21**, 695–703 (2005).
24. S. Khaustova, M. Shkurnikov, E. Tonevitsky, V. Artyushenko, and A. Tonevitsky, *Analyst*, **135**, 3183–3192 (2010); DOI: 10.1039/c0an00529k.
25. D. Perez-Guaita, J. Ventura-Gayete, C. Pérez-Rambla, M. Sancho-Andreu, S. Garrigues, and M. de la Guardia, *Anal. Bioanal. Chem.*, **404**, No. 3, 649–656 (2012).
26. S. A. Khaustova, M. U. Shkurnikov, E. S. Grebenyuk, V. G. Artyushenko, and A. G. Tonevitsky, *Bull. Exper. Biol. Med.*, **148**, No. 5, 841–844 (2009).
27. L. M. Rodrigues, T. D. Magrini, C. F. Lima, J. Scholz, H. da Silva Martinho, and J. D. Almeida, *Spectrochim. Acta A: Mol. Biomol. Spectrosc.*, **174**, 124–129 (2017).
28. D. A. Scott, D. E. Renaud, S. Krishnasamy, P. Meriç, N. Buduneli, S. Cetinkalp, and K. Liu, *Diabetol. Metab. Syndr.*, **2**, 1–9 (2010); DOI: 10.1186/17585996248.
29. C. P. Schultz, M. K. Ahmed, C. Dawes, and H. H. Mantsch, *Anal. Biochem.*, **240**, 7–12 (1996); doi: 10.1006/abio.1996.0323.
30. K. Tsuge, M. Kataoka, and Y. Seto, *J. Heal. Sci.*, **46**, 343–350 (2000).
31. P. Garidel and H. Schott, *Bioproc. Int.*, **1**, 48–55 (2006).
32. P. C. Caetano Júnior, J. Ferreira-Strixino, and L. Raniero, *Res. Biomed. Eng.*, **31**, 116–124 (2015).
33. S. Yoshida and H. Yoshida, *Biopolym.*, **74**, 403–412 (2004); DOi: 10.1002/bip.20072.
34. Z. Movasaghi, S. Rehman, and I. Rehman, *Appl. Spectrosc. Rev.*, **43**, 134–179 (2008).
35. R. R. Sultana, S. N. Zafarullah, and N. H. Kirubamani, *Ind. J. Sci. Technol.*, **4**, 967–970 (2011).
36. J. L. Arrondo and F. M. Goñi, *Chem. Phys. Lipids*, **96**, 53–68 (1998).
37. K. M. Elkins, *J. Forensic Sci.*, **56**, 1580–1587 (2011).
38. Z. Ren, L. D. Do, G. Bechkoff, S. Mebarek, N. Keloglu, S. Ahamada, S. Meena, D. Magne, S. Pikula, Y. Wu, and R. Buchet, *PLoS One*, **10**, e0120087 (2015); https://doi.org/10.1371/journal.pone.0120087.
39. N. Hassler, D. Baurecht, G. Reiter, and U. P. Fringeli, *J. Phys. Chem.*, **115**, 1064–1072 (2011); DOI: 10.1021/jp105870z.
40. M. M. Diaz, O. L. Bocanegra, R. R. Teixeira, S. S. Soares, and F. S. Espindola, *Int. J. Sport Med.*, **34**, No. 1, 8–13 (2013).